Surface segregation near the temperature of bulk phase separation: Incomplete wetting in Cu(Ag) alloys

G. Tréglia
Laboratoire de Physique des Solides, Bâtiment 510, Université de Paris–Sud, 91405 Orsay CEDEX, France

B. Legrand
Section de Recherches de Métallurgie Physique, Centre d'Etudes Nucléaires de Saclay, 91191 Gif-sur-Yvette CEDEX, France

J. Eugène, B. Aufray, and F. Cabané
Laboratoire de Métallurgie, Faculté des Sciences et Techniques Saint-Jérôme, Av. Escadrille Normandie-Niemen, 13397 Marseille, France
(Received 26 November 1990)

Surface segregation in alloys should present drastic modifications near a bulk phase transition. In particular, when the phase diagram exhibits a miscibility gap, one can wonder to what extent surface segregation could be viewed as the first step towards bulk phase separation. We show, in the particular case of very dilute Cu(Ag) alloys, that the actual situation is even more complex. More precisely, using simultaneously an energetic model based on the electronic structure (tight-binding Ising model) and a mean-field approximation formulated as an area-preserving map, we found evidence of incomplete wetting, i.e., a *finite* succession of layering transitions from almost pure Cu to almost pure Ag planes when the bulk Ag concentration approaches the solubility limit. This theoretical result compares satisfactorily with the experimental surface segregation isotherms derived from kinetics studies using Auger-electron spectroscopy, which indeed exhibit, at least, the first (surface) layering transition. Moreover, the experimentally observed hysteresis between the segregation and dissolution isotherms can be interpreted by taking into account the dependence of the size effect with respect to the surface concentration.

I. INTRODUCTION

Surface segregation, i.e., the variation of the composition of an alloy near the surface at thermodynamical equilibrium, has been studied for a long time in relation to its important technological implications (corrosion, catalysis, etc.).[1] From the experimental point of view, the most commonly used tool was Auger-electron spectroscopy[2] (AES) which gives information averaged among the first planes near the surface. Only recently, more sophisticated techniques such as low-energy diffraction[3] (LEED), ion scattering[4] (IS), or time-of-flight (TOF) atom probe[5] have given access to a more detailed knowledge of the concentration profile, i.e., the variation of concentration in planes parallel to the surface. On the other hand, from the theoretical point of view, most of the authors used empirical models, based on a description of the energy in terms of phenomenological pair interactions[6] and only recently have models been developed, derived from the tight-binding formalism, which allow a treatment of surface segregation from the electronic structure.[7]

It is worth pointing out that the great majority of these segregation studies has been performed at a sufficiently high temperature to get a solid solution in the whole range of concentration. This allows a determination of the surface concentration for several finite bulk concentrations at a given temperature in order to draw the equilibrium segregation isotherm giving the surface concentration versus the bulk one.[8] Such a systematics is not possible when the two components of the alloy present very low mutual solubilities. This explains why, except in a few cases,[9] less effort has been devoted to systems for which the phase diagram exhibits a large miscibility gap. Actually, the equilibrium surface segregation must not be confused with a phase precipitation predictable from the phase diagram if the concentration exceeds the solubility limit.[8] In other words, surface segregation can be distinguished unambiguously from phase precipitation for an unsaturated solid solution only, which makes experimental work very difficult when the range of concentration for the solid solution is less than 1%. However, these drawbacks can be counterbalanced by two interesting peculiarities of such systems. The first one is theoretical. On the analogy of adsorption,[10] one easily imagines that surface segregation should vary drastically when the bulk concentration approaches the limit of the miscibility gap. In particular, one can wonder to what extent surface segregation could be viewed as the first step towards bulk phase separation. Similar precursor phenomena have already been observed in the case of surface melting[11,12] or in the case of the wetting by a disordered film of the antiphase boundary between coexisting variants of the ordered structure just below the order-disorder critical temperature.[13,14] The second peculiarity of these low solubility systems is that, experimentally, the systematics with respect to bulk concentration can be replaced by a clever derivation of the equilibrium segregation isotherm from kinetics studies performed for one dilute concentra-

tion only, due to the existence of a local equilibrium in the selvedge of the surface.[15]

Such an experimental work has been performed to study in the same way the segregation of Ag in a very dilute solid solution of Cu(Ag) and the dissolution of an Ag monolayer in a Cu matrix.[16] Both resulting isotherms present, in a very narrow range of temperature, one abrupt step revealing a first-order transition between an almost pure Cu surface and an Ag-rich one. We will show here that a microscopic model based on the electronic structure of the alloy [tight-binding Ising model (TBIM), Sec. II A] (Ref. 7) coupled with a mean-field statistical approach, formulated either as an area-preserving map (APM, Sec. II B) (Ref. 17) or in terms of an effective local field (Sec. II B 2) (Ref. 18), leads in fact to a *finite* succession of layering transitions[12,13,17] from (almost) pure Cu to (almost) pure Ag planes when approaching the miscibility gap limit (Sec. III A). In other words, we predict an incomplete Ag wetting of Cu(Ag) by surface segregation, the first step of which (surface layering transition) is indeed confirmed by experiments (Sec. III B). On the other hand, the experiments also showed an unexpected hysteresis between the segregation and the dissolution isotherms and conclude in the appearance of a (9×9) superstructure when the surface is pure Ag.[16] We will show, using molecular dynamics in a tight-binding scheme (Sec. IV A), that this superstructure is indeed found as energetically the most stable for an Ag surface monolayer (Sec. IV B). Moreover, using an improved treatment of the size-mismatch energy as a function of surface concentration, we can interpret the experimental hysteresis.

II. THEORETICAL MODEL

A. Energetic model: TBIM

A proper electronic structure treatment of surface segregation in transition- and noble-metal alloys would require one to calculate the band grand-canonical energy:

$$\Omega_e(\{p_n^i\})=-\int dE\, f(E)\int_{-\infty}^{E} dE' n(E',\{p_n^i\}) , \quad (1)$$

where $f(E)$ is the Fermi function, $n(E,\{p_n^i\})$ is the electronic density of states corresponding to a given configuration $\{p_n^i\}$ where p_n^i is the occupation number which is equal to 1 or 0 depending on the site n to be occupied by an atom of type i or not. The very complex configuration dependence of the density of states would then forbid one to make statistical mechanics starting from (1). Fortunately, it has been shown recently that the configuration-dependent part of Ω_e could be isolated and written as an effective Ising Hamiltonian:[7]

$$H^{\mathrm{TBIM}}=\sum_{n,i} p_n^i h_n^i+\tfrac{1}{2}\sum_{n,m,i,j}{}' V_{nm}^{ij} p_n^i p_m^j , \quad (2)$$

with

$$h_n^i=\frac{1}{\pi}\mathrm{Im}\int_{-\infty}^{E_F} dE \sum_{\lambda}\ln[1-(\varepsilon^i-\sigma_n)G_{nn}^{\lambda\lambda}(E)] , \quad (3)$$

$$V_{nm}^{ij}=-\frac{1}{\pi}\mathrm{Im}\int_{-\infty}^{E_F} dE\, t_n^i(E)t_m^j(E)\sum_{\lambda,\mu} G_{nm}^{\lambda\mu}(E)G_{mn}^{\mu\lambda}(E) . \quad (4)$$

Here E_F is the Fermi level, ε^i the atomic d level for i atoms and λ,μ the spin-orbital indices ($1\le\lambda,\ \mu\le10$). $G_{nm}^{\lambda\mu}(E)$ is the matrix element $\langle n,\lambda|G|m,\mu\rangle$ of the Green function in the disordered state characterized by the self-energy σ_n described within the coherent-potential approximation[19] (CPA); t_n^i is the corresponding t matrix:

$$t_n^i(E)=\frac{\varepsilon^i-\sigma_n(E)}{1-[\varepsilon^i-\sigma_n(E)]\sum_{\lambda} G_{nn}^{\lambda\lambda}(E)/10} . \quad (5)$$

The prime in Eq. (2) means that the summation involves sites $m\neq n$, with m restricted to first neighbors of n, as previously justified in bulk fcc alloys.[20]

For the binary alloy $Cu_{1-c}Ag_c$ ($p_n=p_n^{Ag}=1-p_n^{Cu}$):

$$H^{\mathrm{TBIM}}=\sum_n p_n\left[h_n-\sum_m{}' V_{nm}\right]+\sum_{n,m}{}' p_n p_m V_{nm} , \quad (6)$$

where the p-layer field ($h_n, n\in p$ layer) and effective pair interaction (V_{nm}) are given by

$$h_n=h_n^A-h_n^B+\tfrac{1}{2}\sum_m{}'\left[V_{nm}^{AA}-V_{nm}^{BB}\right] , \quad (7)$$

$$V_{nm}=\tfrac{1}{2}\left[V_{nm}^{AA}+V_{nm}^{BB}-2V_{nm}^{AB}\right] . \quad (8)$$

The main results of TBIM of practical importance here are the following.[7] First, the difference in layer field between a site belonging to a plane p parallel to the surface ($p=0$ for the surface layer; $p=1$ for the first underlayer, etc.) and a bulk site is numerically identical to the difference in p-layer tensions between pure Ag and pure Cu:

$$\Delta h_p=h_{n\in\text{plane }p}-h_{n\in\text{bulk}}\cong\tau_p^{Ag}-\tau_p^{Cu} . \quad (9)$$

For the (111) surface, it is negligible except in the surface plane where it is given by the difference in surface tensions. It is well known that surface tensions are somewhat underestimated by the tight-binding calculations. To palliate this drawback, we will use here the semiempirical—but reliable—values of Ref. 21. Note, however, that in the particular case of Ag-Cu, both approaches (semiempirical,[21] tight binding[22]) lead to the same numerical value of $\tau_0^{Ag}-\tau_0^{Cu}$:

$$\Delta h_0\cong\tau_0^{Ag}-\tau_0^{Cu}=-110\text{ meV} , \qquad \Delta h_{p>1}\cong0 . \quad (10)$$

In the same spirit, the effective pair interaction V_{nm} is derived from the regular solution parameter,[21]

$$V_{nm}=V=-32\text{ meV} , \quad (11)$$

if sites n and m are bulk sites. According to our TBIM calculations,[7] it is enhanced at the surface,

$$V_{nm}=V_0=1.5\text{ V} , \quad (12)$$

if site n or site m belongs to the (111) surface.

It is important to note that the tight-binding Ising Hamiltonian (2) has been derived on a rigid lattice, neglecting any off-diagonal disorder (for instance, due to size effects). In the presence of a significant size misfit (as it is the case between Cu and Ag), a third contribution has to be introduced which can be written

$$\mathcal{H}^{\mathrm{SE}}=\sum_n p_n \mathcal{H}_n^{\mathrm{SE}} , \tag{13}$$

in which $\mathcal{H}_n^{\mathrm{SE}}$ is the change in energy when a Cu atom is replaced by an Ag atom at a site n of the $Cu_{1-c}Ag_c$ alloy, assuming that Ag and Cu only differ by their atomic radii. This term can be calculated in $Cu(Ag)=Cu(Ag)_{c\to 0}$, i.e., for an Ag impurity in a Cu matrix, by minimizing the strain energy at site n by means of a relaxation process using a quenched molecular dynamics in a tight-binding potential.[22,23] As a result, the segregation energy due to the size mismatch in a plane p parallel to the surface is given by the difference in strain energy between a site of this plane and a bulk site:

$$\Delta\mathcal{H}_p^{\mathrm{SE}}=\mathcal{H}^{\mathrm{SE}}_{n\in \mathrm{plane}\,p}-\mathcal{H}^{\mathrm{SE}}_{n\in \mathrm{bulk}} . \tag{14}$$

For the (111) face of Cu(Ag), one finds that

$$\begin{aligned}&\Delta\mathcal{H}_0^{\mathrm{SE}}=-220\ \mathrm{meV} ,\\ &\Delta\mathcal{H}_{p\geq 1}^{\mathrm{SE}}=0 .\end{aligned} \tag{15}$$

Then the grand-canonical free energy Ω is obtained by averaging the Hamiltonian [(6)+(13)] and the entropic term over all configurations. Using the mean-field approximation and assuming that concentrations only vary for planes p parallel to the surface ($\langle p_n\rangle=c_p\ \forall n\in \mathrm{plane}\,p$), one gets

$$\begin{aligned}\Omega=&\langle H^{\mathrm{TBIM}}\rangle+\langle\mathcal{H}^{\mathrm{SE}}\rangle\\ &+kT\sum_p N_p[c_p\ln c_p+(1-c_p)\ln(1-c_p)]\\ &-\mu\sum_p N_p(c_p-c) ,\end{aligned} \tag{16}$$

where N_p is the number of sites in a p plane and μ is the chemical potential.

B. Statistical mechanics

The problem is now to determine the p-plane concentrations c_p. This is achieved by minimizing the grand-canonical free energy Ω whatever c_p ($\forall p$, $\partial\Omega/\partial c_p=0$), which leads to the following system of coupled nonlinear equations:

$$\forall p,\quad \frac{c_p}{1-c_p}=\exp\{-[\Delta G_p(c_{p-1},c_p,c_{p+1})-\mu]/kT\} , \tag{17}$$

with

$$\begin{aligned}\Delta G_0&=\Delta h_0+\Delta\mathcal{H}_0^{\mathrm{SE}}-(Z+Z')V_0+2V_0(Zc_0+Z'c_1) ,\\ \Delta G_1&=\Delta h_1+\Delta\mathcal{H}_1^{\mathrm{SE}}-(Z'V_0+ZV+Z'V)\\ &\quad+2(Z'V_0c_0+ZVc_1+Z'Vc_2) ,\\ &\cdots ,\\ \Delta G_p&=-(Z+2Z')V+2V(Z'c_{p-1}+Zc_p+Z'c_{p+1}) ,\end{aligned} \tag{18}$$

and the chemical potential given by

$$\mu=\begin{cases}-(Z+2Z')V(1-2c)+kT\ln\dfrac{c}{1-c} & \text{for } T\geq T_c\\ 0 \text{ for } T\leq T_c ,\end{cases} \tag{19}$$

T_c being the critical temperature of phase separation and Z and Z' the numbers of first neighbors of a site in a given bulk layer parallel to the surface in the same plane and in the first plane below (above) respectively. Here, for a (111) face, $Z=2Z'=6$.

One has then to solve the system (17), which can be done by using either an area-preserving mapping of the mean-field approximation[17,18] or a "local-field" relaxation algorithm.[18]

1. *Area-preserving mapping*

The APM technique has been popularized in the field of magnetism by Pandit and Wortis.[17] Nevertheless, its extension to the case of surface segregation with specific boundary conditions (here two, due to the enhancement of V at the surface) is not yet in the current patrimony of surface scientists. This technique has, however, unique abilities when concerned in surface segregation near bulk phase transitions. In particular, it allows one to determine *all* the solutions of system (17) and then the possibility of surface phase transition from one solution to another.[24,25]

The idea is to keep c_{p+1} from the right-hand side of Eq. (17) to express it in terms of c_p, c_{p-1}. This gives

$$\begin{aligned}c_1&=\frac{V}{V_0}[f_1(c_0)-\tfrac{1}{2}]+\frac{1}{2}\left[\frac{V_0}{V}-1\right]\left[1-\frac{Z}{Z'}\left[c_0-\frac{1}{2}\right]\right]\\ &=g_1(c_0) ,\\ c_{p+1}&=f_{p+1}(c_p)-c_{p-1}-\left[\frac{V_0}{V}-1\right](c_{p-1}-\tfrac{1}{2})\delta_{p,1} ,\end{aligned} \tag{20}$$

the f_p function being defined from

$$f_p(x)=\frac{1}{2Z'V}\left[-kT\ln\frac{x}{1-x}-2VZx+(Z+2Z')V-\Delta h_{p-1}-\Delta\mathcal{H}_{p-1}^{\mathrm{SE}}+\mu\right] \tag{21}$$

and the p label being irrelevant for $p\geq 1$ since $\Delta h_{p\geq 1}=\Delta\mathcal{H}_{p\geq 1}^{\mathrm{SE}}=0$ [see Eqs. (10)–(15)]:

$$f_{p\geq 1}(x)=f(x)=\frac{1}{2Z'V}\left[-kT\ln\frac{x}{1-x}-2VZx+(Z+2Z')V+\mu\right] . \quad (22)$$

Therefore Eq. (21) defines the following two-dimensional mapping τ:

$$\begin{bmatrix} c_{p+1} \\ c_p \end{bmatrix}=\begin{bmatrix} f(c_p)-c_{p-1} \\ c_p \end{bmatrix}=\tau\begin{bmatrix} c_p \\ c_{p-1} \end{bmatrix} \quad (23)$$

subject to the appropriate boundary condition(s):

$$c_1=g_1(c_0) ,$$

and if, as usual, $V\neq V_0$, (24)

$$c_2=g_2(c_1)=f(c_1)-g_1^{-1}(c_1)-\left[\frac{V_0}{V}-1\right][g_1^{-1}(c_1)-\tfrac{1}{2}] .$$

The bulk thermodynamics at equilibrium can be described in an elegant way from the number and topological nature of the fixed points of the two-dimensional (2D) mapping defined by (23).[24,25] Let us schematically illustrate in Fig. 1 the changes of the corresponding phase portrait $c_{p+1}(c_p)$ when the concentration increases, at a given temperature T, up to the solubility limit $c_1^{(\infty)}(T)$ which, in a dilute case, can be obtained from Eq. (19):

$$c_1^{\infty}(T)\cong\exp[(Z+2Z')V/kT] . \quad (25)$$

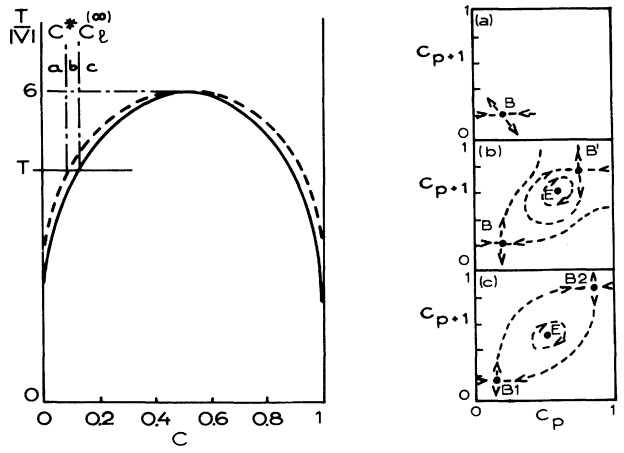

FIG. 1. Left-hand side, bulk phase diagram of an alloy A_cB_{1-c} with negative first-neighbor interactions in the mean-field approximation, illustrating the main regions at a given temperature T: (a) ($c<c^*$), (b) ($c^*<c<c_1^{(\infty)}$), (c) ($c_1^{(\infty)}<c$). Right-hand side, schematic phase portraits corresponding to these main regions.

First [Fig. 1(a)] when c is sufficiently small compared to $c_1^{(\infty)}$, the bulk concentration is the only fixed point $B(c,c)$ of the transformation (23). It is called hyperbolic since linearizing (23) around it leads to real positive eigenvalues λ_1,λ_2 such as $\lambda_1\lambda_2=1$ ($\lambda_1\neq\lambda_2$). The eigenvectors associated to $\lambda_1(<1)$ and $\lambda_2(>1)$ are respectively the slopes of the inflowing orbits (insets) and outflowing orbits (outsets) following the definition given in Ref. [17]. Then [Fig. 2(b)], increasing c, one reaches a value c^*, which for $c_1^{(\infty)}\ll 1$ is given by Ref. 24:

$$c^*(T)\cong c_1^{(\infty)}(T)[-2c_1^{(\infty)}(T)\ln c_1^{(\infty)}(T)]<c_1^{(\infty)}(T) , \quad (26)$$

beyond which two new fixed points B',E appear in addition to $B(c,c)$ which remains the single thermodynamically stable point. $B'(c',c')$ corresponds to a second minimum (less stable than B) in Ω: it is also hyperbolic and develops a homoclinic orbit around the elliptic point E which is a local maximum in Ω. Then when c approaches much more the solubility limit $c_1^{(\infty)}$, c' does the same with respect to $1-c_1^{(\infty)}$, still remaining less stable but with an energy difference decreasing to almost zero. In the same time, the homoclinic orbit of B almost touches the B' point and "horseshoes"[17,26] develop around B'. Finally [Fig. 1(c)], c and c' reach $c_1^{(\infty)}$ and $1-c_1^{(\infty)}$, respectively, with the same value of Ω and the alloy separates into two phases of concentration $c_1^{(\infty)}$ (Cu-rich phase) and $1-c_1^{(\infty)}$ (Ag-rich phase).

We are now able to get the equilibrium concentration profile near the surface from the intersection of the inflowing orbit to B with the boundary condition $c_2=g_2(c_1)$ [Eq. (24)], by keeping its part $(c_1,c_2,\ldots,c_p)$ between the intersection and B and then adding the surface concentration: $c_0=g_1^{-1}(c_1)$. The APM technique therefore allows an easy and physical visualization of the possible existence of multiple solutions in which case the one with the lowest value of Ω should be chosen, a phase transition occurring when a variation of external parameter $(c,T,\ldots)$ switches the minimum value of Ω from one solution to the other.[25] Even though one has to keep in mind that such a variation of c changes in the same time the boundary condition $c_2=g_2(c_1)$ and the insets of B, one imagines from the trends displayed in Fig. 1 that such phase transitions could be easier in the vicinity of the solubility limit. In particular, whether the boundary condition intersects the inset of B in its part which is close to B, or that which is close to B', one can get a concentration profile almost without segregation or with a minority rich region located near the surface, even for concentration lower than the solubility limit. In the latter case, surface segregation could be a precursor step for bulk phase separation.

2. *Local-field relaxation algorithm*

In spite of the appealing character of the APM technique, it could be that, in some very peculiar situations, finding all the possible intersections between the boundary condition and the inset becomes a very tedious task. This should be the case, for instance, in the very vicinity

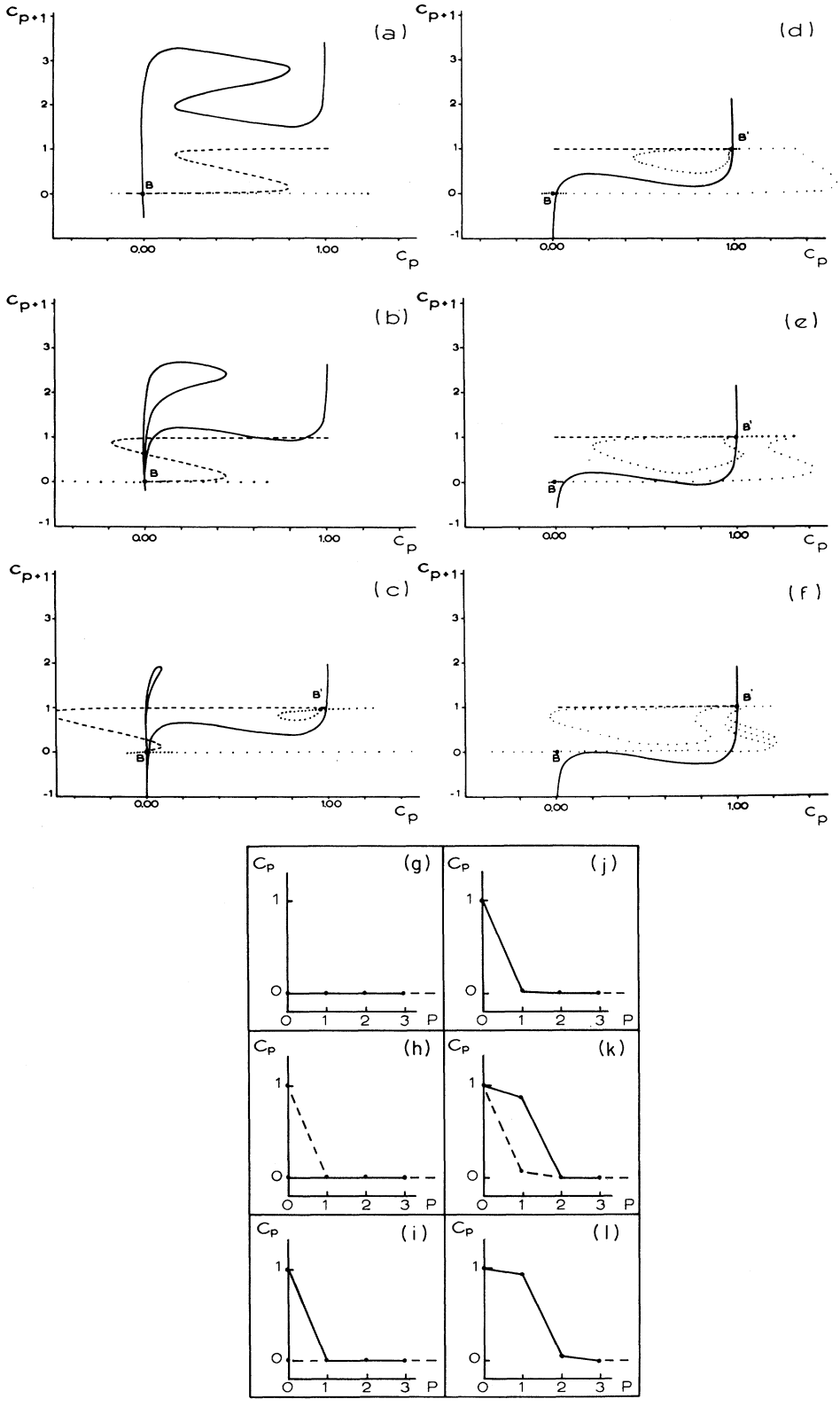

FIG. 2. Phase portraits of $Cu_{1-c}Ag_c(111)$ including the fixed points, their insets ($\cdots$) and the boundary condition $c_2=g_2(c_1)$ (——) as a function of the bulk concentration at $T=750$ K: (a) $c=0.000\,01$, (b) $c=0.000\,05$, (c) $c=0.000\,25$, (d) $c=0.000\,50$, (e) $c=0.0010$, (f) $c=0.0020$ [let us recall that $c_1^{(\infty)}(750\text{ K})=0.0025$]. For convenience, we have also plotted the relation $c_0=g_1^{-1}(c_1)$ (— — —). The corresponding concentration profiles are shown in (g)–(l).

of $c_1^{(\infty)}$, when the boundary condition intersects the horseshoes near B' leading to an infinite number of possible solutions corresponding to $p=1,2,\ldots,\infty$ planes quasipure with respect to the minority element. One has then to imagine a complementary method to compare their relative energies. This is the aim of the local-field relaxation algorithm in which, instead of extracting c_{p+1} from the right-hand side (rhs) of Eq. (17), we choose to extract c_p from its left-hand side (lhs):

$$c_p=\{1+\exp[\Delta G_p(c_{p-1},c_p,c_{p+1})-\mu]/kT\}^{-1} . \quad (27)$$

Thus the relaxation process consists in starting from a given initial set of concentration $\{c_p^{(0)}\}$, then to recalculate all the $c_p^{(1)}$ in their "local field" $\Delta G_p(c_{p-1}^{(1)},c_p^{(0)},c_{p+1}^{(0)})$ or, more generally, at the kth step of the iterative scheme, $c_p^{(k)}$ in its local field $\Delta G_p(c_{p-1}^{(k)},c_p^{(k-1)},c_{p+1}^{(k-1)})$ up to the convergence: $c_p^{(k)}=c_p^{(k-1)},\forall_p$.[18]

III. EQUILIBRIUM CONCENTRATION PROFILE FOR $Cu_{1-c}Ag_c$ WHEN $c\to 0$

A. Theory: incomplete wetting

The evolution of the calculated phase portraits when c increases up to $c_1^{(\infty)}$, at the temperature of experiments [$T=750$ K (Ref. 16)] is shown in Fig. 2. Here, contrary to the schematic description of Fig. 1, we have only plotted the insets of the fitted points, the outsets being not useful for our purpose. One can see that the variation in number and topological nature of the fixed points and of their insets as a function of c indeed follows the trends schematically described in Fig. 1. Let us now discuss in a more precise way the behavior of the boundary condition(s) $c_2=g_2(c_1)$ and $c_0=g_1^{-1}(c_1)$ and of the derived intersections with the inset of B. First, when the concentration is sufficiently lower than the solubility limit [$c\ll c_1^{(\infty)}(750\text{ K})=0.0025$ according to Eq. (25)] the boundary condition intersects the insets of B only once [Fig. 2(a)], the intersection corresponding to $c_2\cong c_1\cong c_0\cong c$, i.e., almost no segregation [Fig. 2(g)]. Then, increasing the concentration while remaining in the range where only one fixed point exists one observes drastic modifications of the boundary condition [see Fig. 2(b)] leading to three intersections: two local minima and one local maximum. The intersections associated with the minima essentially differ by the value of c_0 since $c_1\cong c_2\cong c$ for both of them, whereas $c_0\cong 0$ in one case and $c_0\cong 1$ in the other case. This leads to the concentration profiles exhibited in Fig. 2(h). This bistability remains in a very narrow range of concentration [see Figs. 2(b), 2(h), 2(c), and 2(i)], the stablest solution switching by a first-order transition from the Cu-rich surface to the Ag-rich one for $c\cong 0.0001$. Then, still increasing c beyond c^*, the second (less stable) fixed point B' ($\sim 1,\sim 1$) appears while the boundary conditions still change: in particular, $c_0\cong 1$ whatever c_1 as can be seen in Fig. 2(d). Now, two groups of intersections are found related to B and B', respectively. However, we have to consider the B group only since the other corresponds to a metastable bulk state. This B group reduces to only one profile which is illustrated in Fig. 2(j): a Cu matrix terminated by an Ag surface plane. Then, for larger values of c, the boundary condition intersects three times the insets of B leading to two local minima and one local maximum. The two minima only differ by the value of c_1 (~ 1 or ~ 0) since in both cases $c_0\cong 1$ [see Fig. 2(e)], leading to the concentration profiles of Fig. 2(k): one with two almost pure Ag planes and the other one with only one Ag layer. Here again, the stablest solution switches by a first-order phase transition from the previous solution (one Ag layer) to the new one (two Ag layers) in the concentration range $\cong 0.001-0.002$. Then for $0.002<c<c_1^{(\infty)}(750\text{ K})$, one sees in Fig. 2(f) that only the latter intersection remains up to the very vicinity of $c_1^{(\infty)}$ where the boundary condition intersects the horseshoes near B' leading to multiple intersections with $c_0\cong c_1\cong\cdots\cong c_n\cong 1$ for $n=2,3,\ldots,\infty$, which are almost impossible to separate due to problems of numerical accuracy.

These two first-order transitions can be better visualized by means of segregation isotherms in which we plot, at a given temperature, the quantity of Ag spread in the first two planes: $\theta=c_0+c_1$ as a function of bulk concentration up to the solubility limit. This is the aim of Fig. 3 in which we put in evidence the strong influence of temperature on the existence of such surface phase transitions. Actually, it can be seen that at sufficiently high temperature, the segregation isotherm does not exhibit any first-order transition but instead presents a continuous behavior corresponding to a progressive enrichment of the first two planes with silver. Then decreasing the temperature, the isotherm successively exhibits only one first-order transition (surface layer) and then two such transitions (surface plus first underlayer) as already discussed for $T=750$ K.

In view of this progressive enrichment of the selvedge of the surface by the Ag-rich planes which will phase separate in the bulk beyond the solubility limit, one can

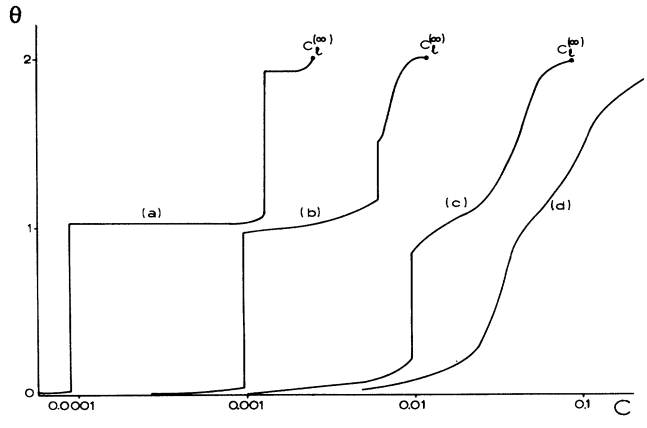

FIG. 3. Theoretical segregation isotherms ($\theta=c_0+c_1$ as a function of c) of $Cu_{1-c}Ag_c(111)$ at different temperatures: (a) $T=750$ K, (b) $T=1000$ K, (c) $T=1500$ K, (d) $T=2000$ K.

wonder to what extent surface segregation in Cu(Ag) could be viewed as a first step towards bulk phase separation. In other words, is there an Ag wetting of the Cu(Ag) surface, i.e., infinite succession of layering transitions from (almost) pure Cu to (almost) pure Ag planes when getting closer and closer to the miscibility gap limit? To answer such a question, one has to solve the numerical problem which arises when the boundary condition intersects the horseshoes of the B inset. In practice, this can be done within the local-field relaxation algorithm described in Sec. II B 2. Indeed, the idea is to start from different initial configurations ($c_0=c_1=1$, $c_2=\cdots c_p=1$, $c_{p+1}=\cdots=c$) for different values of p ($p\geq 2$) and to inquire whether the algorithm keeps a parent configuration as the equilibrium solution. As a result what we find is that for T sufficiently low and c sufficiently close to c_1^{∞}, the concentration profile with $c_2\cong 1$ becomes stabler than the one with $c_2\cong 0$, indeed leading to a third layering transition. On the contrary, even though other concentration profiles with $c_{p\geq 3}\cong 1$ become metastable solutions when getting closer and closer to the miscibility gap limits, the energies of these profiles remain always larger than the energy of the $c_3\cong 0$ profile. As a consequence, one can conclude that what our calculation puts in evidence for Cu(Ag) is an incomplete wetting, i.e., a finite succession of layering transitions (three) from (almost) pure Ag planes when getting closer and closer to the miscibility gap limits. These layering transitions are visualized as new transition lines in the bulk diagram of Fig. 4. Let us now compare these theoretical results to the existing experimental data.[16]

B. Experiments

We will just briefly summarize the experimental method since it is described in detail elsewhere.[16] The main idea is that the equilibrium isotherms (c_0 versus c) can be derived from kinetics studies of segregation or dissolution assuming that there exists some local equilibrium between the surface layer and its selvedge.[15] The experiments have been performed at $T\cong 730$ K by Auger-electron spectroscopy to follow on the one hand the kinetics of segregation of Ag from a solid solution Cu(Ag) (111) and on the other hand the kinetics of dissolution of a monolayer of Ag on Cu(111). The resulting isotherms are shown in Fig. 5. They both exhibit a first-order phase transition which is indeed a layering transition for the dissolution isotherm whereas it is rather a "partial layering transition" for the segregation isotherm. This hysteresis could be understood if one of the driving forces for the Ag enrichment was strongly reduced during the segregation process when the surface concentration reaches a critical value ($c_0\cong 0.5$ according to the breaking in Fig. 5) while it was not affected during the dissolution. From this point of view it is important to note that LEED studies[16] have put in evidence both at the beginning of the dissolution and at the end of the segregation (i.e., for an Ag monolayer at the surface) the existence of a (9×9) superstructure corresponding to a close-packed Ag monolayer on Cu(111).

One can expect, with increasing Ag surface concentration, a decreasing of the size effect term $\Delta\mathcal{H}_0^{SE}$ which accounts for most of the segregation energy when $c_0\rightarrow 0$ (see Table I). Such a possible gradual loss as a function of c_0 has never been considered up to now. We will show in the following that it can indeed explain the hysteresis of Fig. 5.

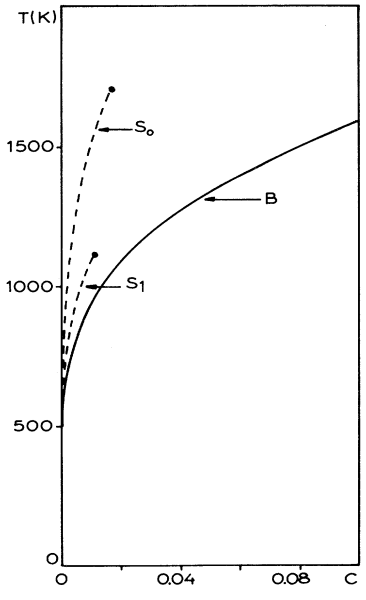

FIG. 4. Mean-field phase diagram of $Cu_{1-c}Ag_c$ including the p-layering transition lines (dashed lines) for $p=1,2,3$. On this scale, the last one is undistinguishable from the bulk line.

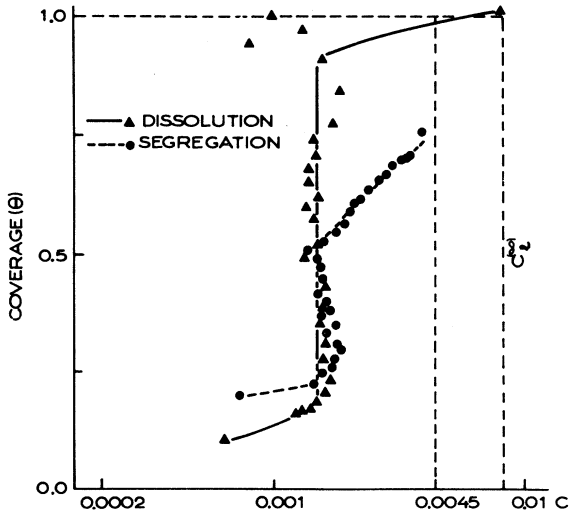

FIG. 5. Experimental isotherms $c_0=f(c)$ derived from segregation and dissolution kinetics at $T\cong 730$ K.

TABLE I. c_0 dependence of the segregation energy ΔH_0, separated into its three components according to (A3).

Structure	c_0	Δh_0 (meV)	$\Delta \mathcal{H}_0^{SE}$ (meV)	ΔH_0^{mix} (meV)	ΔH_0 (meV)	Ref.
(1×1)	0	−110	−220	50	−280	this work
(1×1)	$c_0^l=0.4$	−110	−40	−180	−330	this work
(9×9)	$c_0^l=0.4$	−110	−350	−180	−640	this work
(9×9)	1	−110	−370	−530	−1010	this work
	0	−170	−160	−90	−420	33
	0.4	−170	−160	−250	−580	33
	1	−170	−160	−480	−810	33

IV. MICROSCOPIC TREATMENT OF THE SIZE EFFECT AS A FUNCTION OF THE SURFACE CONCENTRATION

A. Model

Up to now, we have been able to calculate the difference in size-mismatch energy $\Delta \mathcal{H}_0^{SE}$ [Eqs. (13)–(15)] only in the case where both the surface and the bulk are dilute with respect to the impurity. As a consequence, $\Delta \mathcal{H}_0^{SE}$ does not depend on surface concentration so that we will miss any saturation of size effect with c_0 if it exists. This assumed c_0 independence of $\Delta \mathcal{H}_0^{SE}$ is probably incorrect when the solute radius (r_{imp}) is significantly larger ($\geq 10\%$) than the solvent one (r_{mat}) and when surface segregation is sufficiently important to lead to a surface almost pure in the minority element. Indeed, naively speaking, one easily imagines that a big atom is less compressed at the surface than in the bulk when it is surrounded by small atoms but that its situation becomes less and less favorable when the concentration of big atoms increases at the surface. This could even change the sign of ΔH_0^{SE} when c_0 is varied beyond a critical surface concentration. These arguments probably apply to $Cu_{1-c}Ag_c (c \to 0)$ since $r_{Ag} \cong 1.13 r_{Cu}$ and as discussed in the preceding section (Sec. III), the two main factors for surface segregation ($\Delta h_0, \Delta \mathcal{H}_0^{SE}$) lead to an almost pure Ag surface plane at the experimental temperature when $c \geq 0.0001$. It should then be of prime importance in our case to account for a possible c_0 dependence of $\Delta \mathcal{H}_0^{SE}$ in a proper way. This can be done by extending to the case of a finite Ag-surface concentration the microscopic treatment we previously developed for one impurity only.

Let us recall that the tight-binding Ising Hamiltonian (1) has been derived assuming a rigid lattice. To go beyond this assumption, we can add to the band energy (1) a repulsive term E_{rep} of the Born-Mayer type, which was omitted up to now since it is negligible at equilibrium.[27] The total energy can then be written

$$E^{tot}(\{p_n^i\}) = \Omega_e(\{p_n^i\}) + \tfrac{1}{2} \sum_{\substack{n,m,i,j \\ (r_{ij} < r_c)}}{}' p_n^i p_m^j A_{ij} \exp\left[-p_{ij}\left[\frac{r_{ij}}{r_{ij}^0} - 1\right]\right], \tag{28}$$

where A_{ij} and p_{ij} are the usual Born-Mayer parameters determined from the knowledge of the lattice parameter and elastic constants.[22] r_{ij} is the interatomic distance between an atom of type i and another of type j whereas r_{ij}^0 is the sum of the atomic radii. The cutoff radius r_c is taken as an intermediate value between the second-and third-neighbor distances in the matrix. Using then a second moment approximation for the local electronic density of states (which is known to be sufficient in the presence of strong bond relaxation) the band energy in (28) can be rewritten[22,28]

$$\Omega_e(\{p_n^i\}) = -\sum_{n,i} p_n^i \left[\sum_{\substack{m,j \\ (r_{ij} < r_c)}}{}' p_m^j \xi_{ij}^2\right]^{1/2}, \tag{29}$$

where

$$\xi_{ij} = \xi_{ij}^0 \exp\left[-q_{ij}\left[\frac{r_{ij}}{r_{ij}^0} - 1\right]\right]$$

is the effective hopping integral between atoms of type i and j defined in Refs. 18 and 22, q_{ij} is fitted to experimental results in the same way as p_{ij}.

In order to simulate a pure size effect, the cohesive energy of the solute is taken equal to that of the solvent.[22] The size-mismatch energy $\mathcal{H}_p^{SE}$ for an impurity located in the p plane is then obtained from a quenched molecular-dynamics procedure and $\Delta \mathcal{H}_p^{SE}$ is given by Eq. (14). Such a calculation for an Ag impurity in a Cu matrix led to the result given in Eq. (15).

In order to characterize a possible dependence of $\Delta \mathcal{H}_0^{SE}$ with respect to the local concentration c_0 (when $c \to 0$) we have used the same tight-binding quenched molecular dynamics to simulate various sizes of Ag clusters in the surface plane, the Ag additional impurity being located first at the surface, then in the bulk. Note that in this framework, the size effect energy should be written in a more general way as in Eq. (13):

$$\mathcal{H}_0^{SE} = \frac{\partial \mathcal{H}^{SE}}{\partial c_0}. \tag{30}$$

B. Formation of the (9×9) superstructure through the expulsion of atoms induced by size mismatch

In order to allow the relaxation process to stabilize at completion (pure Ag surface) a surface structure in which the Ag atoms could recover their bulk interatomic distances ($r^0_{AgAg}/r^0_{CuCu} \cong \frac{9}{8}$), the molecular dynamics has been performed using $k=6$ mobile (111) layers (on a fixed Cu substrate), each one containing 100 atoms, and the usual periodic conditions. The resulting c_0 dependence of $\Delta\mathcal{H}_0^{SE}$ is nontrivial, as can be seen in Fig. 6. As expected from the previous naive arguments, $|\Delta\mathcal{H}_0^{SE}|$ decreases monotonously up to a critical surface concentration $c_0^l \cong 0.4$. At this concentration, the simulation shows spontaneous jumps of Ag atoms from the surface towards adatom positions. These limited expulsions, which occur when the stress reaches a critical value, reflect the difficult coexistence between "big" and "small" atoms at the surface. As can be seen in Fig. 7(a), this size-mismatch-induced limited expulsion (SMILE) effect allows the remaining Ag surface atoms to reconstruct towards a local superstructure. When the Ag surface concentration is increased, more and more adatoms are expelled from the surface, leading at completion to a full (9×9) superstructure. However, one can wonder to what extent this superstructure, which is indeed the experimental one,[16,29] could be an artifact due to the size of the box used for the simulation. We have checked that this is not the case and that (9×9) superstructure is the stablest epitaxial structure of an Ag monolayer deposited on a Cu(111) substrate. To do that, we have compared the relative stabilities of the different possible $(n\times n)$ superstructures for $n=5$ to 15, the stablest one minimizing the generalized surface energy γ_n:[30]

$$\gamma_n = (E_{tot} - N_{Cu}E^{Cu}_{coh} - N_{Ag}E^{Ag}_{coh})/N \ , \tag{31}$$

where E_{tot} is the energy of a crystallite with N_{Cu} Cu atoms and N_{Ag} Ag ones, N being the number of atoms in a bulk plane parallel to the surface. E^i_{coh} is the cohesive energy of the i metal. In the present case, γ_n can be written explicitly as

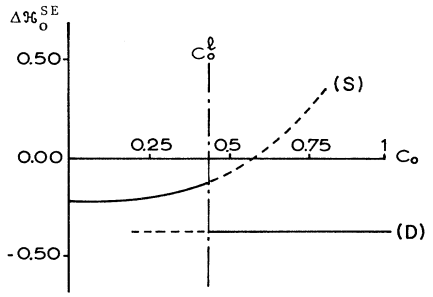

FIG. 6. Surface concentration dependence of the size-mismatch energy $\Delta\mathcal{H}_0^{SE}$ in the dilute bulk concentration limit for a $[Cu_{1-c}Ag_c(111)]_{c\to 0}$ surface presenting either a (1×1) or (9×9) structure. The solid line is for the stable structure, whereas the dashed line is for the metastable one.

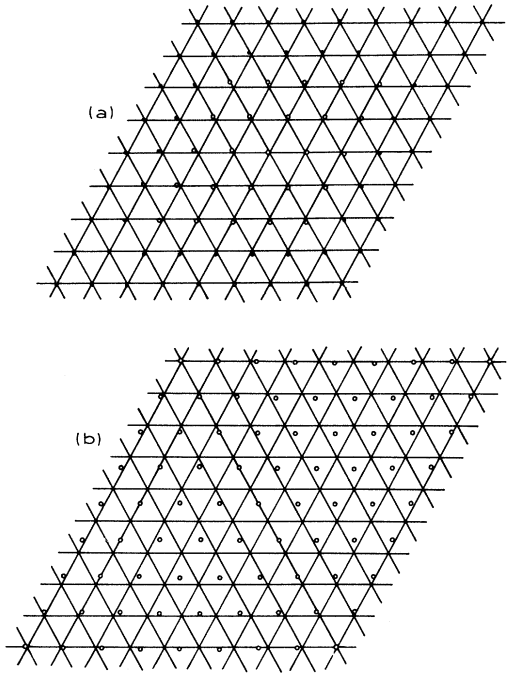

FIG. 7. Theoretical superstructures derived from the numerical simulation for $[Cu_{1-c}Ag_c(111)]_{c\to 0}$ and two surface concentrations: (a) $c_0 \cong 0.25$ and (b) $c_0 = 1$: ●, Cu atoms; ○, Ag atoms.

$$\gamma_n = [E^n_{tot} - (k-1)(n+1)^2 E^{Cu}_{coh} - n^2 E^{Ag}_{coh}]/(n+1)^2 \ , \tag{32}$$

where E^n_{tot} is the total energy of the relaxed structure with $(k-1)$ mobile Cu layers of $(n+1)^2$ atoms and an Ag surface of n^2 atoms. As a result, the structure which minimizes γ_n is indeed the (9×9) one, the minimum being rather flat: $\gamma_{10} \cong \gamma_9$. This good agreement with experimental results could be felt as fortuitous in view of the smallness of the energy differences between competitive structures ($\sim 10^{-2}$ eV/at) and of the apparent simplicity of the energy expression (28), which adds to the tight-binding band term an empirical repulsive one. In fact, this result illustrates once again the surprising predictive ability of this model, already checked in the subtle case of transition-metal surface reconstructions.[28]

Once being granted that the (9×9) superstructure is the stablest surface *at completion,* one can wonder what is its range of stability as a function of the Ag surface concentration, i.e., beyond which critical c_0 is the superstructure stabilized with respect to the (1×1) surface. To answer this question we have compared the relative stabilities of these two structures for the same number of Ag surface atoms using (31). As a result, the (1×1) surface is found the stablest up to the critical concentration c_0^l at which the SMILE effect begins, the (9×9) structure being favored as soon as $c_0 > c_0^l$. This effect can then be identified as the atomic mechanism responsible for pseudoepitaxial dislocation formation. This structural infor-

mation being obtained, we have calculated $\Delta\mathcal{H}_0^{SE}$ for both (1×1) and (9×9) structures, even in the concentration range where they are only metastable. This is illustrated in Fig. 6 where the solid line corresponds to the stable structure [(1×1) for $c_0<c_0^l$, (9×9) for $c_0>c_0^l$] and the dashed line to the metastable one. As can be seen, in the (9×9) structure, $\Delta\mathcal{H}_0^{SE}$ takes values almost independent of c_0 similar to those obtained for the dilute $(c_0\rightarrow0)(1\times1)$ surface.

After completion of this manuscript, we became aware of a paper by Liu and Wynblatt[31] which reports on embedded atom method (EAM)–Monte Carlo simulations performed on the same system. These authors observed that "large Ag atoms are squeezed into previously unoccupied adatom sites," in complete similarity with the present SMILE effect.

C. Hysteresis between segregation and dissolution isotherms

In view of the previous results, one has then to revisit the theoretical segregation isotherm of Cu(Ag), taking into account the c_0 dependence at equilibrium of the size effect displayed in Fig. 6. Assuming that the $(1\times1)\leftrightarrow(9\times9)$ phase-transition mechanism is of nucleation and growth type, one expects (due to the kinetics) the actual c_0 dependence to differ from the equilibrium one, depending on the initial state. In practice, this can be roughly modeled by keeping the metastable parts of the two curves even beyond the critical concentration c_0^l. This leads to the S curve for the segregation process [(1×1) structure] and to the D curve for the dissolution process [(9×9) structure] (see Fig. 6). As can be seen in Fig. 8, whereas the D curve leads to an almost unchanged first layering transition, the S one strongly affects this transition. The influence of the S-type size effect is illustrated in the phase portraits of Fig. 9. The most striking difference with Figs. 2(a)–2(d) comes from the boundary condition (c_0 versus c_1) which jumps from ~0.1 to ~0.3 instead of from ~0 to ~1 [compare Fig. 9(c) to Fig. 2(c)]. As a consequence, the first layering transition is only partial (see Fig. 8), i.e., changes an almost pure Cu surface plane to a mixed Cu-Ag surface which is then progressively enriched with Ag up to $c_0\cong0.6$. The resulting theoretical hysteresis between segregation and dissolution depicted in Fig. 8 is in good agreement with the experimental one shown in Fig. 5 concerning the amplitudes of the transitions. The apparent discrepancy between the critical bulk concentrations (i.e., the concentrations for which the transitions occur) is due to the treatment of the experimental data. In fact, as detailed by Eugène, Aufray, and Cabané in Ref. 16, the relative positions of the isotherms in both processes strongly depend on the precise values of the diffusion coefficients and the authors have chosen to fix this coefficient in order to obtain the same critical bulk concentration for both processes. In view of the present results, this assumption has to be considered with caution.

Finally, let us note that the dependence of the size effect $\Delta\mathcal{H}_p^{SE}$ with local concentration c_p should be considered to model the pth layering transition. This could lead to a decrease of the transition amplitude, and even to a disappearance of the transition. Some work is currently in progress in this direction.

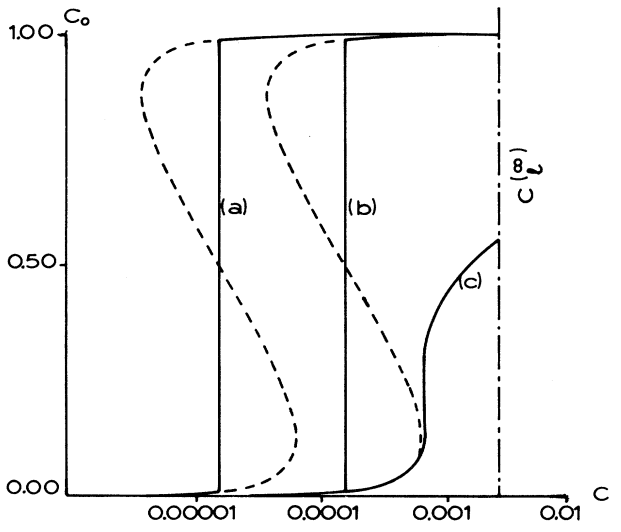

FIG. 8. Theoretical isotherm (c_0 as a function of c) for $Cu_{1-c}Ag_c(111)$ at $T=750$ K calculated using (a) the c_0 dependence of the size-mismatch energy illustrated as the D curve (dissolution) in Fig. 6; (b) the c_0 dependence of the size-mismatch energy illustrated as the S curve (segregation) in Fig. 6; (c) a c_0 independent size-mismatch energy as in Fig. 3.

V. CONCLUSION

Let us summarize the main results of this paper devoted to the theoretical study of surface segregation in dilute Cu(Ag) when the bulk concentration approaches the solubility limit.

(i) Using the TBIM-APM approach in its initial version (i.e., where the size effect does not depend on the *local* concentrations), we have found (when the temperature is not too high) a finite succession of layering transitions (the pth transition switching the pth layer from almost pure Cu to almost pure Ag). This finite character leads to an incomplete wetting of Cu by Ag even at very low temperature. It is worth noticing that such a succession of layering transitions, even though it is now well documented in the adsorption field, was up to now ignored (at least to our knowledge) in classical surface segregation studies. This has to be related to the extensive use, first of monolayer segregation models, then of "trial-error" type methods for solving the set of coupled nonlinear equations. This is one essential advantage of APM to overcome these difficulties.

(ii) In view of the importance of the size effect in Cu(Ag) segregation, we have modeled the dependence of this effect with respect to local concentration, at least for the surface plane. To this aim, we have performed molecular-dynamics simulations which have put in evidence the atomic mechanism which allows one to accom-

modate the stress which increases during the segregation of big atoms (Ag) at the surface. Beyond a critical value of the surface concentration, some big atoms are expelled from the surface plane towards adatom positions. This SMILE effect leads, at the Ag surface completion, to the formation of a (9×9) superstructure.

(iii) Introducing this c_0 dependence in the TBIM-APM treatment drastically modifies the first layering transition in the segregation process. This transition is now found partial (from a quasipure Cu surface to a mixed Cu-Ag one) and asymmetric with respect to $c_0=0.5$. Let us note that such an asymmetry, which comes from the nonlinearity of the c_0 dependence of the size effect, cannot be predicted by usual models.[32,33]

(iv) The experiments[16] performed on this system compare fairly well with our theoretical predictions. First a (9×9) superstructure is indeed observed at the Ag completion of the surface. Then, a first layering transition is put in evidence, which presents a partial and asymmetric character in the segregation process. On the other hand, the experimental hysteresis between the segregation and dissolution processes is attributed to the structural $(1\times1)\rightarrow(9\times9)$ transformation induced by the size effect.

Finally, this study confirms the unique abilities of the simultaneous use of a suitable electronic structure model (TBIM), a powerful method (APM) to solve the set of mean-field nonlinear equations and realistic simulations (tight-binding molecular dynamics) to treat surface segregation, as previously shown in the cases of Cu-Ni,[24] Ag-Ni,[24] Pt-Ni,[25] and Pt-Rh.[34]

ACKNOWLEDGMENTS

The authors gratefully acknowledge F. Ducastelle, A. Khoutami, A. Senhaji, J. Cabané, M. Lagües, and J. P. Biberian for fruitful discussions. They also thank Professor P. Wynblatt for sending them his results before publication.

APPENDIX: EXPRESSION OF THE SEGREGATION ENERGY WITHIN TBIM

The segregation energy ΔH_p of Ag in the plane p of $Cu_{1-c}Ag_c$ is defined by

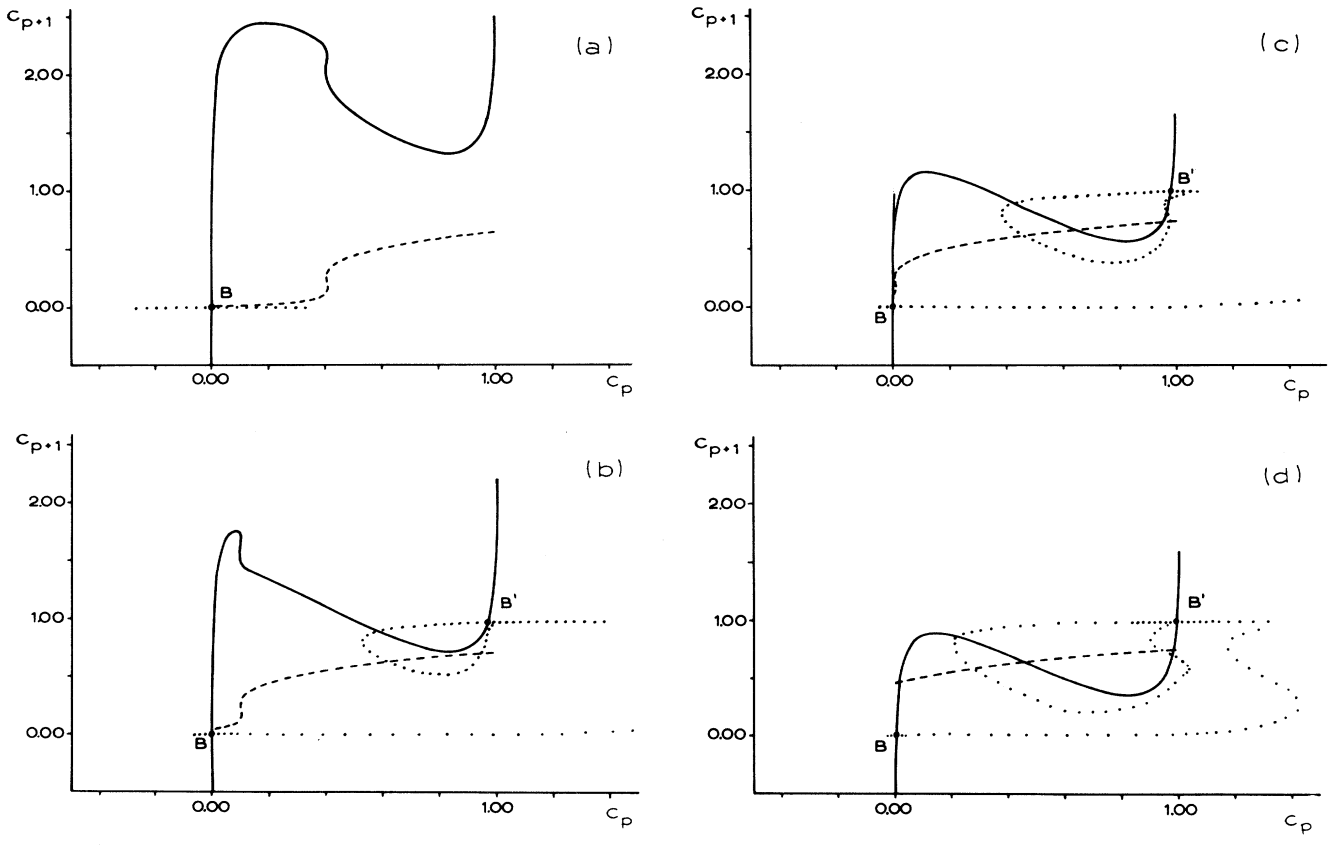

FIG. 9. Phase portraits of $Cu_{1-c}Ag_c(111)$ obtained with the c_0 dependence of the size-mismatch energy illustrated as the S curve in Fig. 6 for (a) $c=0.0001$, (b) $c=0.0003$, (c) $c=0.0006$, (d) $c=0.001$. The notations are the same as in Fig. 2.

$$\frac{c_p}{1-c_p}=\frac{c}{1-c}\exp\left[-\frac{\Delta H_p}{kT}\right] . \quad \text{(A1)}$$

Following Eq. (18) of the main text:

$$\Delta H_p=\Delta G_p+(1-2c)(Z+2Z')V . \quad \text{(A2)}$$

At the surface, the segregation energy ΔH_0 is given by the sum of three terms:

$$\Delta H_0=\Delta h_0+\Delta\mathcal{H}_0^{\mathrm{SE}}(c_0)+\Delta H_0^{\mathrm{mix}} , \quad \text{(A3)}$$

where the first term has been proved[7] to be analogous to the usual surface tension effect, the second term is the surface concentration dependent size effect calculated in Sec. IV and the third term is related to the classical mixing energy:

$$\Delta H_0^{\mathrm{mix}}=(1-2c)(Z+2Z')V-(Z+Z')V_0 +2V_0(Zc_0+Z'c_1) \quad \text{(A4)}$$

which, when interested in the first transition only ($c,c_1\to 0$), can be rewritten:

$$\begin{aligned}\Delta H_0^{\mathrm{mix}}&=(Z+Z')(V-V_0)+Z'V+2V_0Zc_0\\&=V(-1.5+18c_0)\\&=+48-576c_0\ (\text{in meV}) .\end{aligned} \quad \text{(A5)}$$

The respective weights of the three contributions are analyzed in Table I and compared to values used in previous studies.[33]

As can be seen, in the lower part of the segregation isotherm the size effect contribution is the predominant factor when $c_0\to 0$ and almost vanishes when $c_0\to c_0^l$ ($c_0<c_0^l$). Then in the upper part of the isotherm it becomes once again predominant with respect to the surface-tension term. On the other hand, the mixing term, which is negligible at the beginning of the segregation, becomes the leading one near the Ag completion. Concerning the comparison with Ref. 33, it is important to point out that $\Delta\mathcal{H}_0^{\mathrm{SE}}$ in this case has been assumed c_0 independent and calculated when $c_0\to 0$ using the linear continuum elasticity theory.[35,36] It is amusing to note that $\Delta h_0+\Delta\mathcal{H}_0^{\mathrm{SE}}$ has the same numerical value in Ref. 33 and in the present work when $c_0\to 0$ even though each term separately is different due to their different definitions in both theories.[36]

Finally, the experimental value derived from the low part of the isotherm leads to $\Delta H_0^{\mathrm{expt}}\cong -390$ meV (Ref. 33) in good agreement with our theoretical results and in contrast with other calculations performed on this system[33,37] which overestimate this value. This could be due, at least in Ref. 33, to the fact that the surface enchancement of the effective pair interactions [Eq. (12)] has been missed.

[1] J. W. Gibbs, *The Collected Works of J. W. Gibbs* (Yale University Press, New Haven, 1948), Vol. 1; M. P. Seah, Surf. Sci. **80**, 8 (1979); M. J. Kelley and V. Ponec, Prog. Surf. Sci. **11**, 139 (1981); M. J. Sparnaay, Surf. Sci. Rep. **4**, 101 (1984).

[2] F. Pons, J. Le Hericy, and J. P. Langeron, Surf. Sci. **69**, 565 (1977); J. Le Hericy and J. P. Langeron, Le Vide–Les Couches Minces **36**, 205 (1981).

[3] Y. Gauthier, R. Baudoing, and J. Jupille, Phys. Rev. B **40**, 1500 (1989), and references cited therein.

[4] H. H. Brongersma, M. J. Sparnaay, and T. M. Buck, Surf. Sci. **71**, 657 (1978); J. F. Van der Veen, Surf. Sci. Rep. **5**, 199 (1985), and references cited therein.

[5] T. T. Tsong, Surf. Sci. Rep. **8**, 127 (1988).

[6] F. L. Williams and D. Nason, Surf. Sci. **45**, 377 (1974).

[7] G. Tréglia, B. Legrand, and F. Ducastelle, Europhys. Lett. **7**, 575 (1988).

[8] J. M. Blakely and H. V. Thapliyal, in *Interfacial Segregation*, edited by W. C. Johnson and J. M. Blakely (American Society for Metals, Metals Park, OH, 1977), p. 137.

[9] M. G. Barthès and A. Rolland, Thin Solid Films **76**, 45 (1981). A. Rolland, B. Aufray, F. Cabané-Brouty, and J. Cabané, C. R. Acad. Sci. Paris **292**, 1477 (1981); A. Rolland and F. Cabané, Nouv. J. Chim. **8**, 485 (1984); A. Rolland and B. Aufray, Surf. Sci. **162**, 530 (1985); F. Cabané and J. Cabané, J. Phys. (Paris) Colloq. **49**, C5-423 (1988).

[10] R. H. Fowler and E. A. Guggenheim, *Statistical Thermodynamics* (Cambridge University Press, Cambridge, England, 1965); R. Defay, I. Prigogine, A. Bellemans, and D. H. Everett, *Surface Tension and Adsorption* (Longmans, Green, London, 1966); J. M. Blakely and J. C. Shelton, in *Surface Physics of Materials I*, edited by J. M. Blakely (Academic, New York, 1975).

[11] B. Pluis, T. N. Taylor, D. Frenkel, and J. F. Van der Veen, Phys. Rev. B **40**, 1353 (1989); D. M. Zhu and J. G. Dash, Phys. Rev. B **38**, 11 673 (1988); J. F. Van der Veen and J. W. Frenken, Surf. Sci. **178**, 382 (1986); M. Bienfait, J. M. Gay, and H. Blank, *ibid.* **204**, 331 (1988).

[12] R. Lipowsky, Phys. Rev. B **32**, 1731 (1985); S. Dietrich, in *Phase Transitions and Critical Phenomena*, edited by C. Domb and J. Lebowitz (Academic, London, 1987), Vol. 12; E. Tosatti and A. Trayanov, Phys. Rev. Lett. **59**, 2207 (1987).

[13] R. Kikuchi and J. W. Cahn, Acta Metall. **27**, 1337 (1979); A. Finel, V. Mazauric, and F. Ducastelle, J. Phys. Colloq. (Paris) **51**, C1-139 (1990).

[14] A. Loiseau, C. Leroux, D. Broddin, and G. Van Tendeloo, J. Phys. (Paris) Colloq. **51**, C1-233 (1990).

[15] P. Pétrino, F. Moya, and F. Cabané-Brouty, J. Solid State Chem. **2**, 439 (1970); M. Lagües (unpublished); M. Lagües and J. L. Domange, Surf. Sci. **47**, 77 (1975).

[16] J. Eugène, B. Aufray, and F. Cabané, Surf. Sci. **241**, 1 (1991); Y. Liu and P. Wynblatt, Surf. Sci. **241**, L21 (1991).

[17] R. Pandit and M. Wortis, Phys. Rev. B **25**, 3226 (1982).

[18] F. Ducastelle, B. Legrand, and G. Tréglia, Prog. Theor. Phys. Supp. **101**, 159 (1990).

[19] B. Velický, S. Kirkpatrick, and H. Ehrenreich, Phys. Rev. **175**, 747 (1968).

[20] A. Bieber, F. Gautier, G. Tréglia, and F. Ducastelle, Solid State Commun. **39**, 149 (1981).

[21] F. R. de Boer, R. Boom, W. C. N. Mattens, A. R. Miedema, and A. K. Niessen, *Cohesion in Metals* (North-Holland, Amsterdam, 1988).

[22] D. Tomanek, A. A. Aligia, and C. A. Balseiro, Phys. Rev. B **32**, 5051 (1985); V. Rosato, M. Guillopé, and B. Legrand, Philos. Mag. A **59**, 321 (1989).

[23] G. Tréglia and B. Legrand, Phys. Rev. B **35**, 4338 (1987).

[24] G. Tréglia, B. Legrand, and P. Maugain, Surf. Sci. **225**, 319

(1990).
[25]B. Legrand, G. Tréglia, and F. Ducastelle, Phys. Rev. B **41**, 4422 (1990).
[26]V. I. Arnold and A. Avez, *Ergodic Problems of Classical Mechanics* (Benjamin, New York, 1968); S. Aubry, *Structures et Instabilités,* edited by C. Godrèche (Les Editions de Physique, les Ulis, 1985), p. 73.
[27]F. Ducastelle, J. Phys. (Paris) **31**, 1055 (1970).
[28]B. Legrand, G. Tréglia, M. C. Desjonquères, and D. Spanjaard, J. Phys. C **19**, 4463 (1986); Phys. Rev. B **40**, 6440 (1989); M. Guillopé and B. Legrand, Surf. Sci. **215**, 577 (1989); B. Legrand, M. Guillopé, J. S. Luo, and G. Tréglia, Vacuum **41**, 311 (1990).
[29]K. A. R. Mitchell, D. P. Woodruff, and G. W. Vernon, Surf. Sci. **46**, 418 (1974); Y. Namba and R. W. Vook, Thin Solid Films **82**, 165 (1981).
[30]B. W. Dobson, Surf. Sci. **184**, 1 (1987).
[31]Y. Liu and P. Wynblatt, Surf. Sci. **240**, 245 (1990).
[32]J. Du Plessis, Solid State Phenomena **11** (1990).
[33]S. W. Bronner and P. Wynblatt, J. Mater. Res. **1**, 646 (1986).
[34]B. Legrand and G. Tréglia, Surf. Sci. **236**, 398 (1990).
[35]D. McLean, *Grain Boundaries in Metals* (Oxford University Press, London, 1981); J. Friedel, Adv. Phys. **3**, 446 (1954).
[36]P. Wynblatt and R. C. Ku, Surf. Sci. **65**, 511 (1977); in *Interfacial Segregation,* edited by W. C. Johnson and J. M. Blakely (American Society for Metals, Metals Park, OH, 1977), p. 115.
[37]S. M. Foiles, M. I. Baskes, and M. S. Daw, Phys. Rev. B **33**, 7983 (1986).